The 4th European sCO2 Conference for Energy Systems
March 23-24 2021, Online Conference

2021-sCO2.eu-156

ESTIMATED COST AND PERFORMANCE OF A NOVEL SCO2 NATURAL CONVECTION CYCLE FOR LOW-GRADE WASTE HEAT RECOVERY

Kelsi M. Katcher
Southwest Research Institute
San Antonio, TX, USA
Email: kelsi.katcher@swri.org

Michael Marshall
Southwest Research Institute
San Antonio, TX, USA

Natalie R. Smith, Ph.D.
Southwest Research Institute
San Antonio, TX, USA

Cole Replogle
Southwest Research Institute
San Antonio, TX, USA

ABSTRACT

The current work focuses on development of a natural-convection-driven system for low-cost power generation from low-grade heat sources using supercritical carbon dioxide (sCO_2) as the working fluid. Cycle modelling sensitivity studies were conducted to predict available power generation and estimated installation cost for four applications of various thermal and physical scales; the considered applications ranged from a 2 MW-th data center to an 80 MW-th geothermal application. Sensitivity studies included variations in the sCO_2 temperatures and pressures, the flow loop pipe sizing, and the flow loop elevation change to quantify the impact of each design variable on the recoverable power, the thermal efficiency, and the estimated capital cost per power. Results of this study show that increasing the elevation change across the cycle and decreasing low-side CO_2 temperature (to near or below the critical temperature of 31.1°C) generated the most significant improvements in cycle performance and specific cost. It was also found that the cost per power is lowest for the largest thermal scales, namely geothermal-type applications. However, even though the small- and medium-scale applications have higher specific costs, the actual installation cost is still considered relatively low. Therefore, it is expected that these waste heat recovery cycles could still present competitive solutions for small electrical power requirements where very low-grade waste heat is available.

INTRODUCTION

Low-grade heat rejection (at <100-300°C) is commonplace among many industrial, commercial, and residential processes [1], accounting for as much as 80% of total waste heat available [2]. With the broad-reaching push to improve system efficiencies, waste heat recovery (WHR) technologies are gaining more attention. The primary challenge with low-grade heat recovery systems is that the thermal conversion efficiency is inherently very low, resulting in a prohibitively high cost of electricity. Furthermore, most mechanical low-grade WHR installations rely on organic Rankine cycles or Kalina cycles, incorporating single or multiple pumps and expanders for power generation. Utilizing multiple turbomachines drives up system complexity and cost. In addition, process fluid leakage through shaft seals necessitates a makeup/reclamation system, which adds failure points to the system, further increases system cost, and decreases efficiency.

A proposed competitor to these technologies is the natural convection power cycle (or thermosiphon). By utilizing a vertical process loop with heat addition near the bottom and heat rejection near the top, mass flow can be motivated with temperature difference as the only driver (meaning no compressor or pump is required to drive the fluid). Figure 1 depicts the basic arrangement of the natural convection power cycle. The natural convection cycle relies on the differences in hydrostatic pressure between the hot fluid column and the cold fluid column (i.e. pressure equals the product of fluid density, gravity, and the height of the fluid column). If the density of the cold fluid is significantly greater than that of the hot fluid, there will be a net pressure gain across the loop. The achieved mass flow rate is then a function of the hydrostatic pressure gain and the round trip pressure losses, including the operating pressure drop across the power turbine, frictional losses, and minor losses through elbows, valves, heat exchangers, and etc.

The cycle investigated in this study uses supercritical CO_2 (sCO_2) as the working fluid. The fluid properties of sCO_2 are favorable for low-grade WHR because the near-ambient critical point (7.39 MPa and 31.1°C) allows for inherently large density swings near the target waste-heat source temperatures. Furthermore, the high fluid density and relatively low

 DOI: 10.17185/duepublico/73982

viscosities in the supercritical phase allow for minimal frictional losses, increasing the mass flow potential.

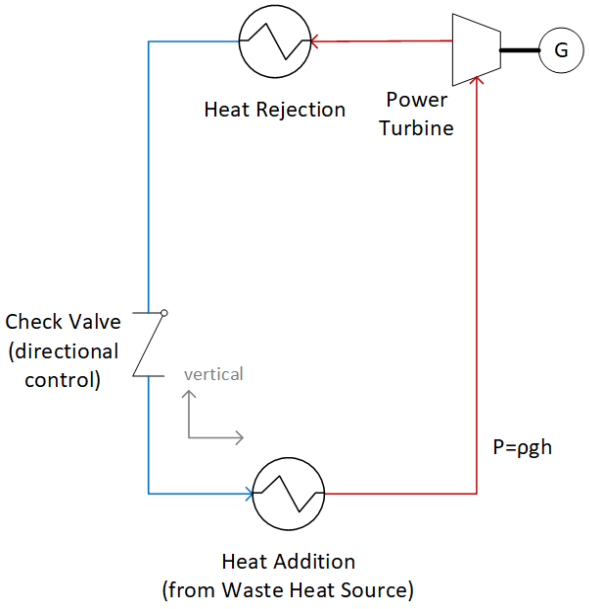

Figure 1: Schematic of natural convection power cycle.

BACKGROUND

Natural convection or thermosiphon loops are commonly used today as secondary fluid systems for heat transfer in applications such as refrigeration, air conditioning, solar collectors, and nuclear reactors. Previous research has shown that sCO_2 can provide increased heat transfer in more compact system when compared to traditional thermosiphons using refrigerants, water, or brine as the working fluid [3,4]. Natural convection work by Sharma (2014) documented Reynolds numbers of up to 10^5 for a CO_2 temperature difference of only 8℃ between the source and sink temperatures, demonstrating the large mass flow potential of CO2 with small changes in temperature [5]. Previous research on sCO_2 natural convection has focused heavily on the heat transfer characteristics of the fluid, showing the complex behavior of local buoyancy effects and localized fluid property gradients (effects that are commonly ignored in traditional cycles, but become significant in a natural convection cycle). Studies have documented large local variations in temperature and axial velocity across the cross section of the pipe [3,4] and large changes in mass flow and heat transfer properties as the fluid approached and crossed the pseudocritical temperature [4,5], the temperature at which the specific heat reaches a local maximum at constant pressure. The high volumetric expansion coefficient and the low viscosity of CO_2 result in strong local buoyancy effects which can cause high radial/azimuthal velocities in the pipe cross-section [4]. This can improve fluid mixing in the heat exchangers, but increased local velocities in the loop cross-section can deter bulk fluid motion around the loop. Therefore, the heat transfer and flow characteristics in the heat exchangers become critical to loop stability [6]. Large deviations from standard heat transfer correlations have also been documented for sCO_2 natural convection. A study by Sharma and Murari (2015) documented that heat transfer coefficients in the fluid show a strong dependence on heat flux at the wall, and that heat transfer deterioration can occur at high heat fluxes [7]. Work by Lei et al. (2017) further explored this phenomenon, showing that a "vapor-like" fluid formed near the pipe wall at high heat fluxes, minimizing the heat transfer from the wall to the bulk fluid (similar to the film boiling phenomenon that occurs at subcritical pressures) [8]. Work by Yadav et al. (2012) proposed modified correlations for heat transfer and friction factor for sCO_2 natural convection, as the measured behaviors did not accurately follow the standard correlations [4].

Substantially less work has been documented on applying sCO_2 natural convection for power generation. A MW-scale sCO_2 thermosiphon was considered for geothermal power generation, utilizing a semi-open-loop cycle composed of separate injection and production wells where the working fluid flows through the rock strata [9-10]. Supercritical CO_2 thermosiphons for geothermal have gained increasing interest because the low viscosity allows for improved flow through the rock strata as compared to traditional thermosiphons operating with supercritical water. A second team presented a closed-loop sCO_2 cycle with the injection and production pipes running in a U-configuration in the same well [11]. Both concepts present utility-scale power generation capabilities.

In previous work by this team, it was found that a thermosiphon can be achieved at various source temperatures and various thermal scales [12]. When operating near the critical point, significant mass flow rates can be achieved with relatively small temperature deltas across the sCO_2 streams. A sensitivity study was conducted to understand the relative impact of the various cycle and loop parameters; changes in the hot CO_2 temperature, cold CO_2 temperature, CO_2 pressure, pipe diameter, and loop height were considered. It was found that the most significant power gains could be achieved by increasing the loop height and by decreasing the cold-side CO_2 temperature. Decreasing the cold-side temperature was found to have significantly more potential than increasing the hot-side temperature; for the loop size investigated, decreasing the cold-side CO_2 temperature from 34°C to 28°C improved the power output by the same amount as increasing the hot-side CO_2 temperature from 100°C to 140°C [12]. The highest values for available power were predicted when the cold-side CO_2 temperature was below the critical temperature (dropping the CO_2 into a pressurized liquid state). Furthermore, the achievable power increases with loop mass flow. Therefore, decreasing the pressure losses is critical for cycle performance. The previous study also quantified the pressure rise across the cycle that could be utilized across the power turbine. It was found that the pressure is expected to be relatively constant throughout the loop, so a low-head power turbine design is required for power conversion.

In general, the capital cost as well as operating and maintenance (O&M) costs must be minimized to make low-grade WHR economical and practical. To better understand the capabilities of the sCO_2 natural convection power cycle for low-grade WHR, a sensitivity study was performed to predict cycle performance and capital cost for four waste heat applications of various thermal and physical scales.

NATURAL CONVECTION CYCLE MODEL

A cycle model was developed to predict the fluid properties of the natural convection cycle. Inputs to the model include CO_2 hot-side and cold-side temperatures, pipe diameter, and linear pipe lengths (including piping and heat exchanger lengths). The pipe loop was assumed to be rectangular (four elbows) with a check valve just upstream of the heater and the power turbine just upstream of the cooler. The flow loop was discretized, and fluid properties were calculated at each node. The NIST REFPROP equations of state were used to calculate the fluid properties of the CO_2.

As a starting point, CO_2 pressure and temperature were defined at the power turbine outlet. From the turbine outlet, the pressure and temperature deltas were calculated between nodes around the cycle. Pressure deltas were calculated as the sum of the change in hydrostatic pressure (using fluid density and elevation change), the frictional losses through the piping and heat exchangers (using flow density, velocity, Reynolds number, friction factor, and piping dimensions), and the minor losses through pipe fittings and the check valve (using fluid density and velocity). In the current model, the vertical pipe runs were considered isothermal, and the heat exchangers were defined by the CO_2 outlet temperatures. In order to achieve the maximum pressure-gain across the cycle, the temperature differences (and density differences) must be maintained across the vertical legs of the loop; for this reason, it is assumed that the loop is insulated and the vertical legs would be near isothermal. The change in temperature due to change in pressure is expected to be relatively small for all above-ground cycles considered here; for the largest cycle the temperature is predicted to change by less than 1.5°C assuming constant enthalpy across the vertical leg. For the geothermal cycle, the change in CO_2 temperature with pressure will be more significant over the large elevation change. However, from the current literature, it is unclear how well-insulated the injection and recovery wells can be. Therefore, an isothermal assumption was used as a starting point for this cost analysis. Furthermore, in previous work by this team, it was found that the cycle performance is highly dependent on the heat exchanger performance and heat exchanger model. Because the heat exchanger geometries will be system-specific and a point of optimization, the heater and cooler in this model were defined by specifying the CO_2 outlet temperature at each.

An iterative, numerical solver was used to select the CO_2 mass flow rate that would satisfy the energy balance in the loop. Namely, this mass flow balances the pressure gain across the cycle with the total pressure loss, as well as matches the starting fluid properties at the power turbine exit to those at the end of the cycle calculation (closing the loop). The pressure and enthalpy drop across the turbine were calculated using an isentropic efficiency value, specified by the turbine sizing calculations (summarized below). The solver was also setup to select the expander outlet pressure that would maximize power output; cycle performance is sensitive to the selected operating pressure [12]. A cycle trade study was used to calculate the head drop across the power turbine and the isentropic power for various temperature combinations and various pipe loop dimensions.

LAB- SCALE NATURAL CONVECTION VALIDATION

The developed cycle model was validated using a lab-scale natural convection test loop (see the constructed loop presented in Figure 2). The test loop was constructed using 1-inch stainless tubing and a height of approximately 4.5 meters. Heat addition and rejection were accomplished through a hot-water bath and an ice bath, respectively. The test loop utilized an orifice plate to simulate the pressure loss across a power turbine. The test loop was operated at varied conditions. The conditions for one steady-state operating point are summarized in Table 1. At this condition, the hot water bath temperature was 65.4°C, and the ice bath temperature was 12.9°C. Note that the cold-side CO_2 temperature dropped well below the critical temperature; therefore, a phase change was occurring in each heat exchanger. The measured mass flow rate was relatively constant, and no cycle instabilities were seen. Based on these results, all subsequent cycle designs considered a cold-side CO_2 temperature near or below the critical temperature.

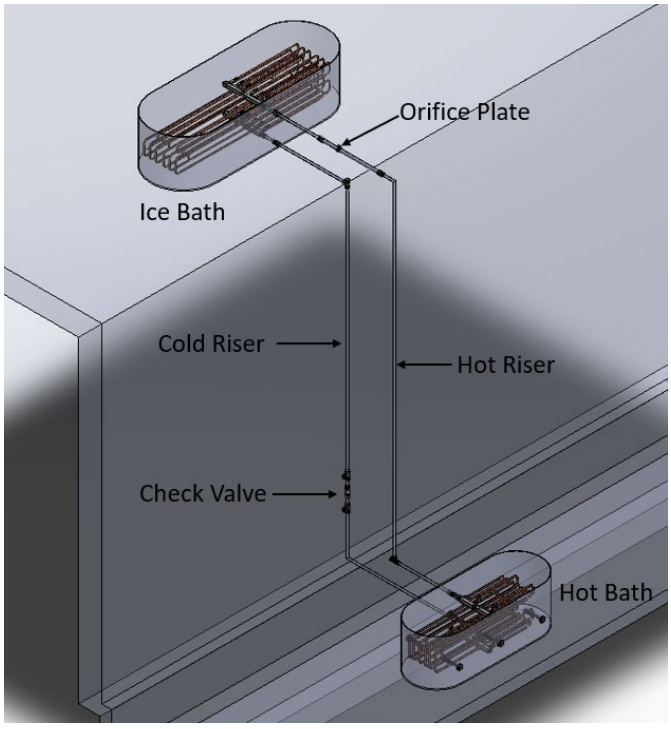

Figure 2: Lab-scale natural convection test loop

Table 1: Lab-scale natural convection test loop steady-state operating conditions

CO_2 Conditions	Cooler Outlet	Heater Outlet
Temperature (°C)	16.0	48.1
Pressure (MPa)	8.768	8.784
Density (kg/m^3)	870.3	281.7
Mass Flow (kg/s)	0.143	

Note that the pressure change across the cycle is quite small. The maximum pressure difference is measured between the top of the hot-side vertical pipe (8.761 MPa) and the bottom of the cold-side vertical pipe (8.795 MPa). With this small change in pressure, a mass flow rate of 0.143 kg/s was achieved. This corresponded to a fluid velocity of 1.08 m/s at the expected turbine location.

METHODS

To evaluate the performance and capital cost of the natural convection cycle, a trade study was performed on four target waste-heat applications to quantify the impact of temperature, pipe size, and loop height. The four waste-heat applications selected were

(1) 2 MW-th data center,
(2) 4 MW-th data center,
(3) 10 MW-th industrial, and
(4) 80 MW-th geothermal.

The temperature range and loop sizes selected were intended to be representative of each specific application. Using the developed cycle model, the isentropic power was calculated for each loop configuration. Thermal efficiency was calculated as the isentropic power over the thermal input. A capital cost was also estimated for each configuration using defined cost functions for the various components. Cost functions are defined in the following sections. Note that the presented cost functions simplify the true capital cost of the various components, and are meant to represent general trends that can be used for understanding how the natural convection loop cost trends with scale. These cost trends are expected to be relatively accurate within the range of values presented, but should not be extrapolated outside what is presented in this study.

Turbine Cost Function

For each application, the inlet and outlet conditions for the power turbine were predicted using the cycle model. These conditions were run through a turbine sizing code based on radial turbine experience charts [13,14] to determine basic turbine sizing. See all values summarized in Table 2. For the first three waste-heat applications, a single stage turbine was sized due to the low available head rise. Multi-stage designs in these applications would operate at even lower speeds with smaller impeller diameters. For the geothermal turbine, sizing sweeps were conducted for rotational speeds of 5,000 to 30,000 RPM and one- to five-stage machines. The turbine design with the best isentropic efficiency was a single-stage machine operating at 20,000 RPM.

The turbine sizing analysis was used to estimate the capital cost of the power turbine for a natural convection cycle. The turbine design for the first three applications was assumed to utilize a sealed concept with immersed bearings and a magnetic coupling to minimize complexity and reduce cost at the smaller scale [15]. The geothermal power turbine design is expected to be similar to sCO_2 power turbines designed in previous work based on the head, rotational speed, and size [15]. The turbine cost model considered the cost of stock material, machining, and welding for the impeller and the housing; connection flanges; instrumentation connections; and the coupling. Based on the turbine sizing and the estimated fabrication costs, it was found that the turbine cost trended best with turbine power. The following turbine cost function was used for this study.

$$\text{Cost (USD)} = 227.10 * P + 23{,}288.47$$

where P is the isentropic turbine power in kilowatts.

Table 2: Radial turbine sizing for each waste-heat application

Application	1	2	3	4
Mass Flow (kg/s)	12.65	18.00	28.94	230.0
Inlet				
Temperature (°C)	66.6	76.3	200.0	210.0
Pressure (MPa)	8.70	8.55	8.37	20.00
Enthalpy (kJ/kg)	461.22	480.14	638.31	611.51
Entropy (kJ/kg-K)	1.83	1.89	2.28	2.08
Exit				
Temperature (°C)	65.9	75.8	198.7	133.7
Pressure (MPa)	8.619	8.50	8.24	8.50
Enthalpy (kJ/kg)	490.92	479.93	637.33	559.71
Entropy (kJ/kg-K)	1.83	1.89	2.28	2.08
Turbine Sizing				
Speed (RPM)	2,500	1,100	3,000	20,000
Impeller Diam. (mm)	138.0	316.7	206.9	210.0
Isentropic Efficiency	76.2%	95.0%	78.9%	95.6%

Heat Exchanger Cost Function

The heat exchanger cost function was developed using vendor quotes sourced for various sCO_2 applications. All quotes represent heat exchangers that are pressure- and temperature-rated for the target conditions. Quotes were for a mixture of water-cooled and air-cooled heat exchangers. See quotes summarized in Figure 3 as a function of thermal duty. Based on these data, a linear cost function was used

$$\text{Cost (USD)} = 70 * Q$$

where Q is the rated thermal duty of the heat exchanger in kilowatts.

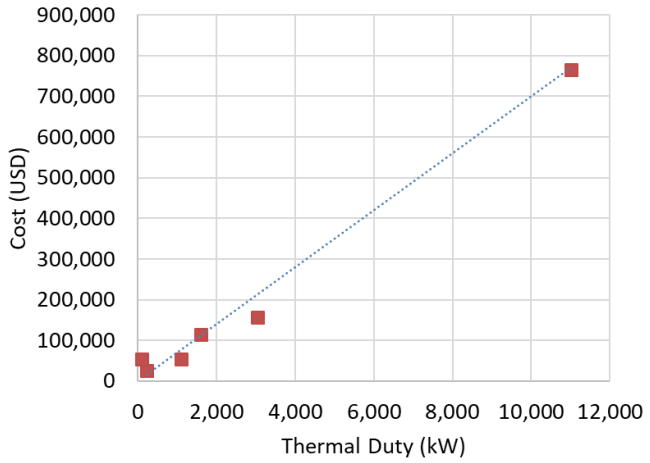

Figure 3: Summary of heat exchanger quotes used to define cost function.

Pipe Cost Functions

The linear pipe cost was segmented based on pipe size and rating. The minimum required pipe wall thickness was calculated using the methods detailed in the ASME B31.1 Power Piping Code. For the smaller scale applications where a very large elevation gain is not achievable (as in applications 1 through 3), the peak pressure in the cycle is very near the critical point. For this reason, a design pressure of 12 MPa was used to choose the minimum piping thickness. Stainless steel pipe was assumed for the increased corrosion resistance with sCO_2. For pipe sizes below 1.5-inch NPS, schedule 5 piping is sufficiently rated. For pipe sizes up to 3.5-inch NPS, schedule 10 piping is sufficient. For pipe sizes up to 12-inch NPS, schedule 40 piping is sufficient. The pipe sizing breaks and the estimated linear piping cost per length are presented in Figure 4.

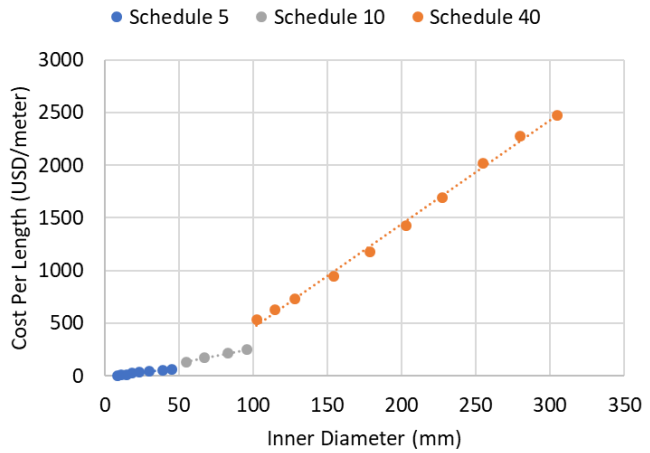

Figure 4: Linear cost function, pipe schedule selected using ASME B31.1 power piping code.

The associated linear cost functions (in U.S. dollars per meter) for each pipe schedule are

Schedule 5	Cost = 1.54 * ID – 4.18
Schedule 10	Cost = 2.81 * ID – 18.03
Schedule 40	Cost = 9.87 * ID – 531

where ID is the inner pipe diameter in millimeters.

The piping flange cost was accounted for separately. For pipe sizes below 1.5-inch NPS, a flat cost of 383.33 USD was used. For larger pipe sizes, the following cost function was utilized.

$$\text{Cost (USD)} = 0.049 * \text{ID}^2 - 0.65 * \text{ID} + 312.82$$

where ID is the inner pipe diameter in millimeters. This cost function assumes 900# ANSI raised-face flanges. This flange rating is sufficient at these pressures and temperatures, but at higher operating temperatures a higher flange rating will be required. For this study, it was assumed that six flanges will be required, one at each connection for the heat exchangers and the turbine.

The elbow costs were also accounted for separately. For pipe sizes below 1.5-inch NPS, the elbow cost was calculated as

$$\text{Cost (USD)} = 0.40 * \text{ID} + 11.19$$

where ID is the inner pipe diameter. For larger pipe sizes, the elbow cost was calculated as

$$\text{Cost (USD)} = 0.038* \text{ID}^2 – 2.14 * \text{ID} + 23.00,$$

again, where ID is the inner pipe diameter.

The costs used here to estimate the cost functions for the linear pipe, the flanges, and the elbows were based on historical pricing and supplier quotes for stainless steel piping and fittings.

Power Generation/Conversion Cost Function

This cost function accounts for the cost of the generator and power conversion equipment to move from mechanical power to useable electrical power. Generator quotes were sourced for multiple sizes from three vendors. Vendor quotes were also collected to estimate the baseline cost for a rectifier, capacitors, inverter module, and a DC/DC module. Note that the power conversion setup must be customized for each specific application to suit the power output needs and the power generation scale. However, this cost was included as an estimate for the electrical power conversion. The following cost function was utilized in this study.

$$\text{Cost (USD)} = 0.106 * \text{P} + 3407.70$$

where P is the turbine power output in watts.

Geothermal Cost

It is expected that the cost functions presented here scale suitably for the first three applications (2 MW-th to 10 MW-th). However, it is expected that the cost of the geothermal application may be higher than what these cost functions will predict. The higher pressure turbine inlet pressure and higher rotational speeds present additional challenges with the turbine shaft and casing designs. Furthermore, drilling and casing a well is expected to be more costly than the sum of linear piping and a typical heat exchanger. For this reason, 20% additional cost was added to the value predicted using these simple linear cost functions.

RESULTS & DISCUSSION

Within this section, results of the trade study performed for each application are summarized. The input parameters, predicted isentropic turbine power, isentropic thermal efficiency, capital cost, and cost per power are presented for multiple configurations considered for each application.

(1) 2 MW-th Data Center

The 2 MW-th data center application considered heat rejection from data center servers with a thermal load of 2 MW. In a new installation, the cooling passages among the server racks could be built integral to the natural convection system, such that the CO_2 is providing direct cooling. Alternatively, the natural convection loop could be installed as a secondary system in which cooling air rejects heat from the servers and then an air-CO_2 heat exchanger cools the air before it is recycled through the servers. This installation would be well-suited for a data center retrofit.

Nine cycle configurations are presented here. The input conditions considered are presented in Table 3. In this study, the cold-side and hot-side CO_2 temperatures were held constant. All combinations of three pipe diameters and three loop heights were considered.

Table 3: Cycle input conditions for 2 MW-th data center

Config.	T-cold (°C)	T-hot (°C)	Pipe ID (mm)	Height (m)
1	30.0	66.6	154.1	15
2	30.0	66.6	202.8	15
3	30.0	66.6	254.3	15
4	30.0	66.6	154.1	20
5	30.0	66.6	202.8	20
6	30.0	66.6	254.3	20
7	30.0	66.6	154.1	25
8	30.0	66.6	202.8	25
9	30.0	66.6	254.3	25

Consistent with previous results, the highest available power and thermal efficiency are predicted for the natural convection loop with the highest elevation change (Figure 5). Among the cases with the same loop height, peak power and efficiency were achieved when the largest pipe size was used (minimizing pressure losses and increasing mass flow). As expected, the capital cost of the natural convection loop increases with loop height and pipe size (Figure 6). However, the lowest cost per power is predicted for configuration 7, which has the largest loop height but the smallest pipe size. This result shows that the additional power output gained by increasing the loop height offsets the increased linear piping cost. However, the power output gained by increasing the pipe size does not offset the increase piping cost (including linear pipe, flanges, and elbows).

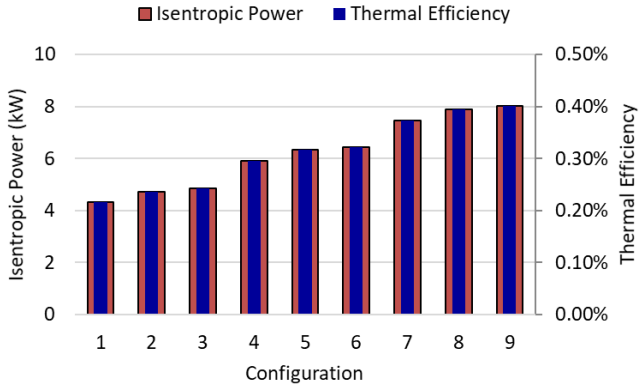

Figure 5: Cycle performance predictions for 2 MW-th data center

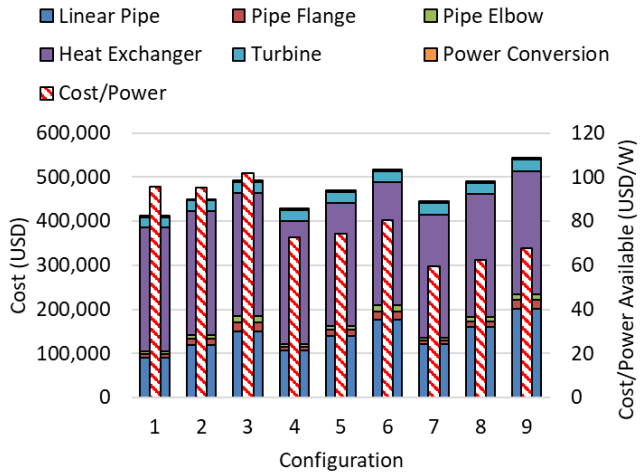

Figure 6: Capital cost predictions for 2 MW-th data center

Configuration 7 is considered the best case of those presented here. This configuration utilized a loop height of 25 meters and a pipe diameter of 154.1 mm (6-inch NPS). For CO_2 temperatures of 30.0°C and 66.6°C, an isentropic turbine power of 7.46 kW was predicted yielding a thermal efficiency of 0.37%. The predicted capital cost is $444,494; the predicted cost per power is $59.57/W. See the steady-state cycle operating point for configuration 7 presented in Table 4.

Table 4: Steady-state cycle operating conditions for 2 MW-th data center, configuration 7

CO_2 Conditions	Cooler Inlet	Cooler Outlet	Heater Inlet	Heater Outlet
Temperature (°C)	65.4	30.0	30.0	66.6
Pressure (MPa)	7.5111	7.5108	7.6714	7.6708
Density (kg/m^3)	164.7	662.4	678.4	168.1
Enthalpy (kJ/kg)	474.0	291.4	288.4	474.2
Mass Flow (kg/s)	11.06			
Isen. Power (kW)	7.46			

(2) 4 MW-th Data Center

The 4 MW-th data center application is the same as the previous case, differing only by the thermal load. Eleven cycle configurations are presented. The input conditions are summarized in Table 5. For this trade study, the loop height was held constant. Three CO_2 temperature combinations were considered with various pipe sizes.

Consistent with previous results, the highest power and thermal efficiencies were predicted for the configurations utilizing the lowest CO_2 cold-side temperature and the largest pipe sizes (Figure 7). For the second temperature combination (30.0°C and 66.6°C), power gains did not increase significantly for pipe diameters greater than 254.3 mm. At this point, the frictional losses through the piping have been minimized, so further increasing pipe size presents no benefit.

As expected, the capital cost of the loop increases with pipe size (Figure 8). The lowest cost per power is predicted for the configurations utilizing the lowest cold-side CO_2 temperature. In this study, smaller pipe sizes were considered to determine the cost per power minimum for fixed temperature conditions. The lowest cost per power is predicted for configuration 6, which has a cold-side CO_2 temperature of 30.0°C, a hot-side temperature CO_2 of 66.6°C, and a pipe diameter of 254.3 mm. At smaller pipe sizes, the cost per power value is predicted to significantly increase because the produced power decreases as the frictional losses through the piping become larger.

Table 5: Cycle input conditions for 4 MW-th data center

Config.	T-cold (°C)	T-hot (°C)	Pipe ID (mm)	Height (m)
1	35.0	66.6	303.0	20
2	35.0	66.6	333.2	20
3	35.0	66.6	381.0	20
4	35.0	66.6	428.8	20
5	30.0	66.6	202.8	20
6	30.0	66.6	254.3	20
7	30.0	66.6	303.0	20
8	30.0	66.6	333.5	20
9	30.0	66.6	381.0	20
10	35.0	70.0	333.3	20
11	35.0	70.0	381.0	20

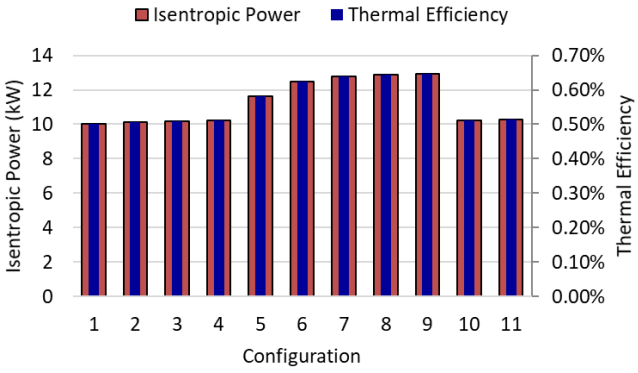

Figure 7: Cycle performance predictions for 4 MW-th data center

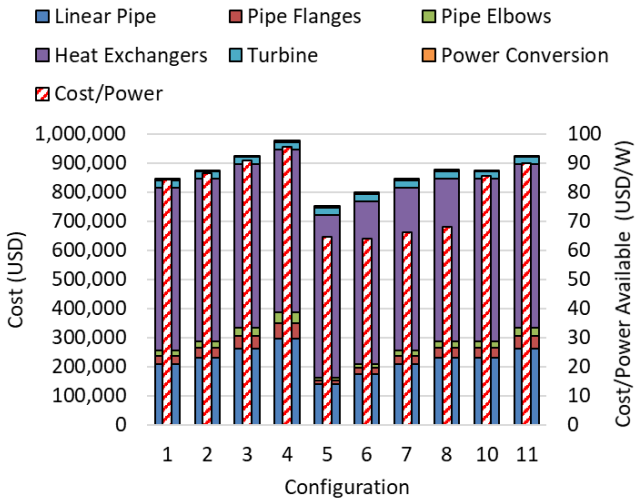

Figure 8: Capital cost predictions for 4 MW-th data center

Configuration 6 is considered the best case of those presented here (see Table 6). This configuration utilized a loop height of 20 meters and a pipe diameter of 254.3 mm (10-inch NPS). For CO_2 temperatures of 30.0°C and 66.6°C, an isentropic turbine power of 12.5 kW was predicted yielding a thermal efficiency of 0.62%. The predicted capital cost is $799,712; the predicted cost per power is $64.00/W.

Table 6: Steady-state cycle operating conditions for 4 MW-th data center, configuration 6

CO_2 Conditions	Cooler Inlet	Cooler Outlet	Heater Inlet	Heater Outlet
Temperature (°C)	65.6	30.0	30.0	66.6
Pressure (MPa)	7.4880	7.4879	7.6166	7.6163
Density (kg/m^3)	164.6	659.6	673.5	166.3
Enthalpy (kJ/kg)	474.7	291.9	289.3	474.8
Mass Flow (kg/s)	22.12			
Isen. Power (kW)	12.50			

(3) 10 MW-th Industrial

This application considered heat rejection from an industrial process with a substantial heat load of 10 MW-th. An industrial facility is expected to have a large building that can support a tall natural convection loop; a loop height of 25 meters was considered. The hot-side heat exchanger would be specific to the heat rejection application, but the cold-side heat exchanger was assumed to be a finned-tube array exposed to ambient air. The cold-side CO_2 temperature was held at 32°C for this trade study, as the cooling potential would be limited by the ambient air conditions. Ten cycle configurations are presented. Hot-side CO_2 temperatures of 120°C and 200°C were considered with varied pipe sizes (Table 7).

Table 7: Cycle input conditions for 10 MW-th industrial application

Config.	T-cold (°C)	T-hot (°C)	Pipe ID (mm)	Height (m)
1	32.0	120.0	406.4	25
2	32.0	120.0	355.6	25
3	32.0	120.0	323.9	25
4	32.0	120.0	273.1	25
5	32.0	120.0	219.1	25
6	32.0	200.0	406.4	25
7	32.0	200.0	355.6	25
8	32.0	200.0	323.9	25
9	32.0	200.0	273.1	25
10	32.0	200.0	219.1	25

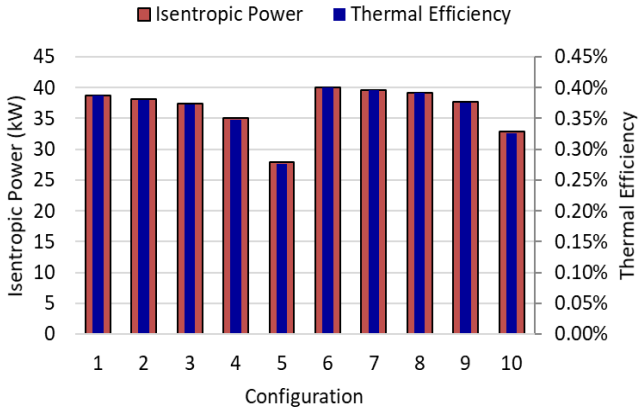

Figure 9: Cycle performance predictions for 10 MW-th industrial application

Consistent with previous results, the highest available power and thermal efficiency are predicted for the natural convection loop with the largest pipe size and the highest CO_2 hot-side temperature (Figure 9). As expected, the capital cost of the natural convection loop increases with pipe size (Figure 10). The lowest cost per power is predicted for configuration 8 (see Table 8), which utilizes a hot-side CO_2 temperature of 200°C and a pipe diameter of 323.9 mm (12-inch NPS). This configuration yielded an isentropic turbine power of 39.2 kW and a thermal efficiency of 0.39%. The predicted capital cost is $1.727M; the predicted cost per power is $44.08/W.

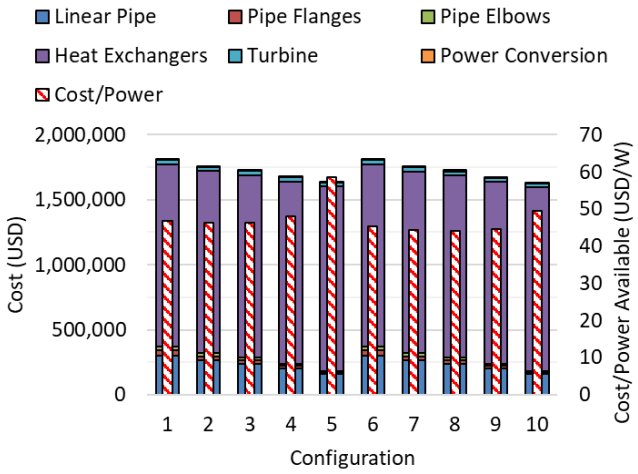

Figure 10: Capital cost predictions for 10 MW-th industrial application

Table 8: Steady-state cycle operating conditions for 10 MW-th industrial application, configuration 8

CO_2 Conditions	Cooler Inlet	Cooler Outlet	Heater Inlet	Heater Outlet
Temperature (°C)	198.4	32.0	32.0	200.0
Pressure (MPa)	8.1869	8.1868	8.3505	8.3502
Density (kg/m^3)	99.0	669.9	682.1	100.6
Enthalpy (kJ/kg)	637.1	293.0	290.7	638.4
Mass Flow (kg/s)	28.93			
Isen. Power (kW)	39.17			

(4) 80 MW-th Geothermal

This application considered a geothermal application using a fully closed-loop well, meaning the downhole piping acts as the heat exchanger and the CO_2 does not directly contact the formation. An elevation change of 2,300 meters and a lateral length of 1,000 meters were assumed for this study. Cold-side and hot-side CO_2 temperatures of 25°C and 240°C were utilized for all configurations. Six configurations were considered with pipe size varying from 16-inch NPS to 34-inch NPS. See the cycle input parameters summarized in Table 9.

In this study, it was found that the peak power and thermal efficiency were achieved at the larger pipe sizes (Figure 11). However, these larger pipe sizes significantly increase the capital cost and the cost per power (Figure 12). The lowest cost per power was actually predicted for the smallest pipe size considered (configuration 1). Configuration 1 (see Table 10) yielded an isentropic turbine power of 13.35 MW and a thermal efficiency of 16.7%. The predicted capital cost is $38.09M; the predicted cost per power is $2.85/W.

Table 9: Cycle input conditions for 80 MW-th geothermal application

Config.	T-cold (°C)	T-hot (°C)	Pipe ID (mm)	Height (m)
1	25.0	240.0	381.0	2300
2	25.0	240.0	428.8	2300
3	25.0	240.0	478.0	2300
4	25.0	240.0	574.5	2300
5	25.0	240.0	777.8	2300
6	25.0	240.0	828.6	2300

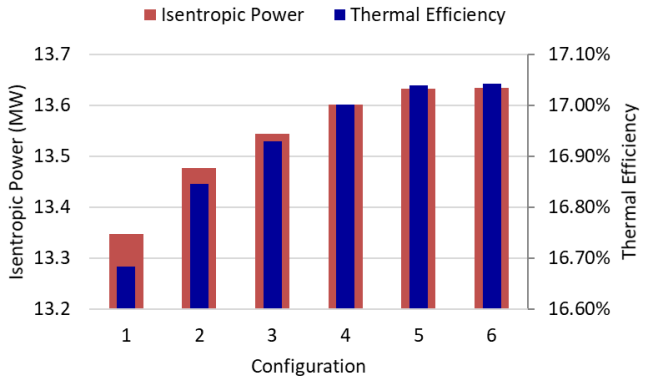

Figure 11: Cycle performance predictions for 80 MW-th geothermal application

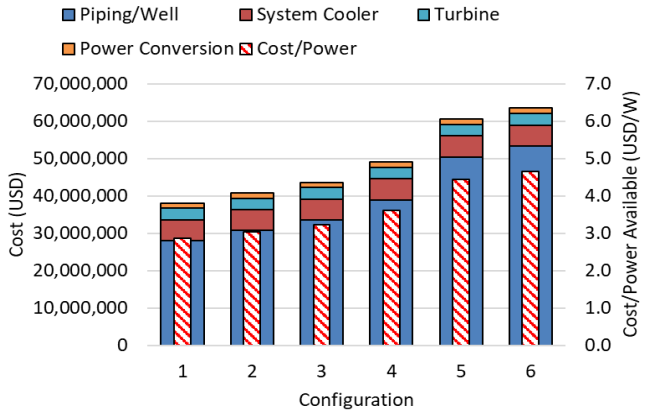

Figure 12: Capital cost predictions for 80 MW-th geothermal application

Table 10: Steady-state cycle operating conditions for 80 MW-th geothermal application, configuration 1

CO_2 Conditions	Cooler Inlet	Cooler Outlet	Heater Inlet	Heater Outlet
Temperature (°C)	151.7	25.0	25.0	240.0
Pressure (MPa)	7.4000	7.3830	24.3830	24.3800
Density (kg/m^3)	102.9	757.9	939.8	275.9
Enthalpy (kJ/kg)	586.9	266.3	242.4	640.7
Mass Flow (kg/s)	190.23			
Isen. Power (kW)	13,346.21			

Scale Comparison

The capital cost is predicted to increase with the waste-heat thermal duty (Figure 13). The capital cost steps up two orders of magnitude from the 2 MW-th case to the 80 MW-th case. However, this study also shows that the specific capital cost per power significantly reduces with increased waste-heat load. This is due to the significant increase in power output with increased thermal scale. When comparing the first three cases (2 MW-th to 10 MW-th), the predicted power increases with thermal duty at about the same rate as the capital cost. There was a much more significant increase in power output between the 10 MW-th case and the 80 MW-th geothermal case (relative to the increase in capital cost); this is expected to be due to the increased thermal duty as well as the significantly larger elevation change in the loop. It is expected that the increased elevation change also significantly improved the thermal efficiency (to 16.7%), as the thermal efficiency predicted for the first three cases was relatively constant (between 0.37% and 0.62%).

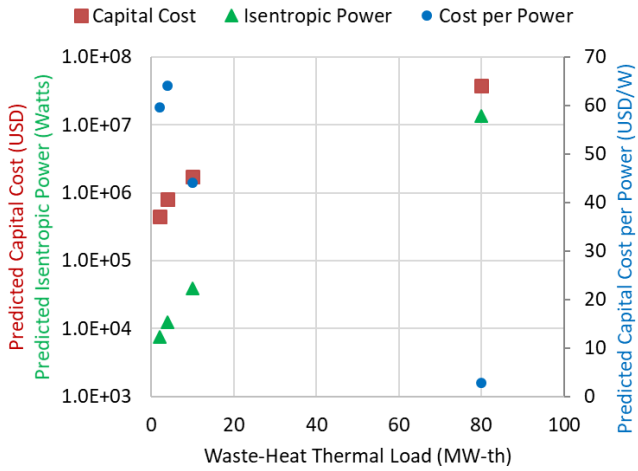

Figure 13: Capital cost and power output predictions for various thermal scales

CONCLUSIONS

In this study, it was found that a natural convection cycle can produce significant levels of power utilizing only waste heat and a single turbomachine. The performance was found to vary with thermal scale, CO_2 conditions, and loop sizing. These results were consistent with the results of previous studies. Here, it was also found that the capital cost is expected to follow the trends of cycle power, namely capital cost increases with pipe size, loop height, and CO_2 temperature delta. However, it was found that the specific capital cost per power did not necessarily follow these trends. In general, it was found that cost per power decreased with increasing loop height, meaning the additional power output gained by increasing the loop height offsets the increased linear piping cost. It was also found that the pipe size should be optimized for the target operating conditions. Increasing the pipe size above the

optimum increases cost without improving power; at this point the frictional losses in the piping have gone to zero, so further increasing diameter presents no power gains. However, using a pipe size below the optimum increases the frictional losses (limiting mass flow and power output), which decreases capital cost but increases the cost per power. In general, the capital cost per power can be minimized by increasing elevation change across the loop, reducing CO_2 cold-side temperature, and selecting an intermediate pipe size.

It was found that the cost per power also decreases with thermal duty. Increasing the amount of heat transfer to the natural convection cycle increases density change across the cycle, in turn increasing pressure gain, mass flow, and power output. The thermal efficiency was also predicted to improve at larger thermal scales. As the performance improves, the cost per power is driven down. This poses the geothermal application at a competitive cost point of 2.85 dollars per watt-electric for utility-scale power generation. This also meant that the smaller thermal scales have a relatively high cost per power, but it should be noted that the total capital cost is relatively low (well below $1M for the smallest scales presented). Furthermore, the heat exchanger cost was predicted to make up the largest portion of the capital cost for the smaller-scale applications. Simplifying heat exchanger design for the target applications could further reduce the capital cost for a natural convection cycle installation.

The natural convection cycle calculations showed that significant power levels can be produced using CO_2 hot-side temperatures as low as 67°C; this could translate to waste-heat applications with source temperatures well below 100°C. These results show that the thermal efficiency and power increase proportionally with loop height and thermal load more significantly than with hot-side temperature, separating this cycle from the typical organic Rankine and Kalina cycles. If a substantial pressure gain can be achieved across the loop, high source temperatures are not required.

It is understood that the thermal efficiencies for the natural convection cycle at smaller scales are low. However, the system simplicity and the cycle's ability to operate in a self-sustaining and passive manner allow this technology to be competitive in very low-grade waste heat applications where the efficiencies of organic Rankine cycles and Kalina cycles cannot compete because the cost per power becomes too high. The simplicity and compactness of the natural convection power cycle make this an attractive option for building retrofit for residential, commercial, and industrial energy recovery.

NOMENCLATURE

ID	Inner pipe diameter
MW-th	megawatt thermal
NPS	nominal pipe size
P	isentropic turbine power
Q	rated thermal duty
sCO_2	supercritical carbon dioxide
T	temperature
USD	United States dollars
WHR	waste heat recovery

ACKNOWLEDGEMENTS

This project was funded and supported by the Southwest Research Institute Internal Research & Development program.

REFERENCES

[1] United States Department of Energy. (2015). Waste heat Recovery Technology Assessment.

[2] BCS, Incorporated. (2008). Waste Heat Recovery: Technology and Opportunities in the U.S. Industry. U.S. Department of Energy, Industry Technologies Program.

[3] Chandra, R.R. (2017). A study on Carbon-dioxide Based Thermosyphon Circulation Loop with End Heat Exchangers. International Journal for Research in Applied Science & Engineering Technology (IJRASET), vol. 5, pp. 1721-1726.

[4] Yadav, A.K., Gopal, M.R., and Bhattacharyya, S. (2012) CO2 based natural circulation loops: New correlations for friction and heat transfer. International Journal of Heat and Mass Transfer 55, pp. 4621-4630.

[5] Sharma, M. (2014) Investigation into steady state and stability behavior of natural circulation systems operating with supercritical fluids. Tokyo Metropolitan University. Japan, Tokyo.

[6] Chen, L., Zhang, X.R., Cao, S., and Bai, H. (2012) Study of trans-critical CO2 natural convection flow with unsteady heat input and its implications on system control. International Journal of Heat and Mass Transfer, vol 55, pp. 7119-7132.

[7] Sharma, D. and Murari, P.K. (2015) Computational Study of Effect of Increasing Heat Flux on Convective Heat Transfer in Sub Channels of Carbon Dioxide Flow at Pressure Above Critical Value. Applied Mechanics and Materials, vol. 772, no. 1662-7482, pp. 8-13.

[8] Lei, X., Zhang, Q., Zhang, J., and Li, H. (2017). Experimental and Numerical Integration of Convective Heat Transfer of Supercritical Carbon Dioxide at Low Mass Fluxes. Applied Sciences, vol. 7, issue. 12, no. 1260.

[9] Atrens, A.D., Gurgenci, H., and Rudolph, V. (2009). CO2 Thermosiphon for Competitive Geothermal Power Generation. Energy & Fuels, vol. 23, pp. 553-557.

[10] Gurgenci, H., (2015). Options to Use Solar Heat to Enhance Geothermal Power Plant Performance. Proceedings World Geothermal Congress, Melbourne, Australia.

[11] Higgins, B.S. and Oldenburg, C.M. (2016). Process Modeling of a Closed-Loop sCO2 Geothermal Power Cycle. The 5th International Supercritical CO2 Power Cycles Symposium, San Antonio, TX, USA.

[12] Katcher, K. M., Allison, T., Marshall, M., and Smith, N. R. (2020). Low-Cost, Low-Grade Waste Heat Recovery Using sCO2 Natural Convection. Proceedings of the 7th

International Supercritical CO2 Power Cycles Symposium. San Antonio, Texas, USA.
[13] Balje, O. E. (1981). Turbomachines: A Guide to Design Selection and Theory. John Wiley & Sons, New York.
[14] Aungier, R. H. (2000). Centrifugal Compressors: A Strategy for Aerodynamic Design and Analysis. ASME Press.
[15] Nielson, J.T., Smith, N.R., Katcher, K.M., Allison, T.A., Marshall, M. (2021) Novel Power Conversion to Utilize sCO2 Natural Convection for Low-Grade Waste Heat Recovery. Proceedings of ASME Turbo Expo 2021.

DOI: 10.17185/duepublico/73982
URN: urn:nbn:de:hbz:464-20210330-124412-5